Received: 12 June 2023 | Revised: 11 September 2023 | Accepted: 12 October 2023

DOI: 10.1002/prot.26622

RESEARCH ARTICLE

PROTEINS WILEY

Secondary structure and toxicity of lysozyme fibrils are determined by the length and unsaturation of phosphatidic acid

Abid Ali[1] | Kiryl Zhaliazka[1] | Aidan P. Holman[1] | Dmitry Kurouski[1,2]

[1]Department of Biochemistry and Biophysics, Texas A&M University, College Station, Texas, USA

[2]Department of Biomedical Engineering, Texas A&M University, College Station, Texas, USA

Correspondence
Dmitry Kurouski, Department of Biochemistry and Biophysics, Texas A&M University, College Station, TX 77843, USA.
Email: dkurouski@tamu.edu

Funding information
National Institute of General Medical Sciences

Abstract

A progressive aggregation of misfolded proteins is a hallmark of numerous pathologies including diabetes Type 2, Alzheimer's disease, and Parkinson's disease. As a result, highly toxic protein aggregates, which are known as amyloid fibrils, are formed. A growing body of evidence suggests that phospholipids can uniquely alter the secondary structure and toxicity of amyloid aggregates. However, the role of phosphatidic acid (PA), a unique lipid that is responsible for cell signaling and activation of lipid-gated ion channels, in the aggregation of amyloidogenic proteins remains unclear. In this study, we investigate the role of the length and degree of unsaturation of fatty acids (FAs) in PA in the structure and toxicity of lysozyme fibrils formed in the presence of this lipid. We found that both the length and saturation of FAs in PA uniquely altered the secondary structure of lysozyme fibrils. However, these structural differences in PA caused very little if any changes in the morphology of lysozyme fibrils. We also utilized cell toxicity assays to determine the extent to which the length and degree of unsaturation of FAs in PA altered the toxicity of lysozyme fibrils. We found that amyloid fibrils formed in the presence of PA with C18:0 FAs exerted significantly higher cell toxicity compared to the aggregates formed in the presence of PA with C16:0 and C18:1 FAs. These results demonstrated that PA can be an important player in the onset and spread of amyloidogenic diseases.

KEYWORDS
amyloid fibrils, LDH, lysozyme, phosphatidic acid

1 | INTRODUCTION

Although the exact molecular cause of amyloid diseases is unknown, a growing body of evidence shows that these pathologies are linked to a progressive aggregation of misfolded proteins.[1–4] Microscopic analysis of protein deposits revealed the presence of long unbranched aggregates with both flat and twisted morphologies, which were named amyloid fibrils.[5,6] Solid-state nuclear magnetic resonance (NMR) and cryoelectron microscopy were able to resolve the secondary structure of these aggregates.[7,8] It was found that amino acid sequences of proteins were folded in a dry-zipper β-sheet structure that was propagating microns in length.[5,9–12] These β-sheet filaments could intertwine or associate side-by-side with other filaments building higher-order structures known as proto-fibrils and fibrils.[13,14] Microscopic analysis also revealed that in addition to fibrils, amyloid deposits contained fragments of plasma membranes or even entire endosomes.[15] This observation suggests that lipid membranes could play an important role in the aggregation of misfolded proteins.[16,17]

Galvagnion et al. demonstrated that lipid vesicles could alter the aggregation rate of α-synuclein (α-Syn), small proteins that were linked to Parkinson's disease.[18,19] It was also found that with an increase in the concentration of lipid vesicles relative to the

concentration of the protein an increase in the rate of α-Syn was observed. However, with a subsequent increase in lipid to protein ratio, a decrease in the aggregation rate of the protein was observed. Galvagnion et al. proposed that surfaces of lipid vesicles could act as templates for protein association.[18,19] Thus, as the small concentration of vesicles, their small surface area relative to the concentration of protein facilitates protein–protein interactions. However, with an increase in the vesicle concentration, the probability of such interactions decreases. Zhaliazka et al. discovered that the charge of lipids played a crucial role in the dynamics of protein aggregation.[20] Specifically, all negatively charged phospholipids, such as phosphatidylserine (PS) and cardiolipin (CL), strongly accelerated the aggregation rate of lysozyme, whereas lipids with net neutral charge (zwitterions) strongly suppressed protein aggregation.[20] Similar findings were recently reported by Matveyenka et al. for insulin.[21,22] The researchers also found that not only the net charge but also the structural properties of fatty acids (FAs) in such phospholipids could play an important role in the stability of amyloidogenic proteins.[21,23,24] Specifically, it was found that large unilamellar vesicles (LUVs) of unsaturated CL enabled a much greater acceleration of insulin aggregation compared to the LUVs with saturated CL.[21] Our group also found that the length of FAs in addition to their saturation could alter the rate of insulin aggregation. Specifically, we found that insulin in the presence of PS LUVs with 14-carbon atom long FAs exhibited a much shorter lag phase compared to PS with 18-carbon atom long FAs.[23] It is important to emphasize that these structural differences in phospholipids not only caused changes in the aggregation rate of insulin and lysozyme but also yielded structurally different oligomers and fibrils if were present during protein aggregation.[21–26]

Phosphatidic acid (PA) is a negatively charged phospholipid that plays an important role in activation of lipid-gated ion channels.[27,28] Unlike other phospholipids, PA does not possess the head group, whereas its *sn*-1 and *sn*-2 positions are typically esterified to saturated and unsaturated FAs.[29] Although PA constitutes only ∼0.25% of plasma membranes, it is highly abundant in lung surfactant.[30,31] In the membranes, PA's unique geometry allows for the precise control of membrane fusion and fission steps, which are highly important for the vesicle trafficking.[32] Recently, Matveyenka et al. found that PA could uniquely alter the aggregation rate of insulin.[24] Furthermore, the change in the insulin aggregation rate directly depends on the length and saturation of FAs in PA.[24] Specifically, PA with palmitic acids (saturated FAs with 16 carbons $C_{16:0}$, PA-$C_{16:0}$) inhibited insulin aggregation, whereas PAs with stearic acids (18 carbons $C_{18:0}$ FAs, PA-$C_{18:0}$) and oleic acid (unsaturated FAs with one double bond $C_{18:1}$ FAs, PA-$C_{18:1}$) strongly accelerated the rate of insulin aggregation. It was also found that insulin aggregates grown in the presence of PA-$C_{16:0}$ exerted significantly lower cell toxicity than insulin fibrils formed in the presence of PA-$C_{18:0}$ and PA-$C_{18:1}$. The question to ask is how general is reported by Matveyenka et al. finding on the length- and saturation-determined effect of PA to other amyloidogenic proteins.

To answer this question, we investigate the secondary structure and toxicity of lysozyme fibrils formed in the presence of PA-$C_{16:0}$, PA-$C_{18:0}$, and PA-$C_{18:1}$. Our results showed that both length and saturation of PA uniquely altered the secondary structure of lysozyme fibrils, as well as toxicity that these aggregates exert to N27 rat neuronal cells.

2 | MATERIALS AND METHODS

2.1 | Materials

Chicken-egg lysozyme was purchased from Sigma-Aldrich (St. Louis, MO, USA), 1,2-dipalmitoyl-sn-glycero-3-phosphate (16:0/16:0-PA, PA-$C_{16:0}$), 1,2-dioleoyl-sn-glycero-3-phosphate (18:1/18:1-PA, PA-$C_{16:1}$), and 1,2-distealoyl-sn-3-phosphate (18:0/18:0-PA, PA-$C_{18:0}$) were purchased from Avanti (Alabaster, AL, USA).

2.2 | Liposome preparation

To prepare LUVs of PA-$C_{16:0}$, PA-$C_{18:0}$, and PA-$C_{18:1}$, 0.6 mg of each lipid was dissolved in 2.6 mL of phosphate-buffered saline (PBS), pH 7.4. Next, solutions were heated ∼50°C for 30 min using a water bath. After that, samples were immersed into liquid nitrogen for 3–5 min. The thawing-heating cycle was repeated 10 times. To homogenize size of lipid vesicles, lipid solutions were passed through 100 nm membrane using extruder (Avanti, Alabaster, AL, USA). Finally, we utilized dynamic light scattering to ensure that the size of the LUVs was within 100 ± 10 nm.

2.3 | Lysozyme aggregation

In the lipid-free environment, 200 μM of lysozyme was dissolved in PBS; solution pH was adjusted to pH 3.0 using concentrated HCl. For PA-$C_{16:0}$, PA-$C_{18:0}$, and PA-$C_{18:1}$, 200 μM of lysozyme was mixed with an equivalent concentration of the corresponding PA; pH of the final solution was adjusted to pH 3.0 using concentrated HCl. Next, samples were placed into heat-block that was agitated with 510 rpm for 24 h. Temperature for all samples was 65°C.

2.4 | Atomic force microscopy imaging

We used AIST-NT-HORIBA system (Edison, NJ, USA) of atomic force microscopy (AFM) to perform morphological analysis of protein aggregates. For AFM imaging, silicon tapping-mode AFM probes Appnano (Mountain View, CA, USA) were used. Force constant was 2.7 N/m; resonance frequency was 50–80 kHz. For each measurement, an aliquot of the sample was diluted with distilled water (DI) water and placed on the surface of precleaned glass coverslip. After 20–30 min exposition, the excess of solution was removed from the glass surface. Finally, coverslips were dried under the flow of dried nitrogen. Preprocessing of the collected AFM images was made using AIST-NT software (Edison, NJ, USA).

2.5 | Circular dichroism

After 24 h of incubation at 65°C, samples were diluted to the final concentration of 100 μM using PBS and measured immediately using Jasco J1000 circular dichroism (CD) spectrometer (Jasco, Easton, MD, USA). Three spectra were collected for each sample within 190–250 nm and averaged. Spectra were acquired with 1 nm spectral resolution.

2.6 | Attenuated total reflectance Fourier-transform infrared spectroscopy

After 24 h of incubation at 65°C, samples were placed onto attenuated total reflectance crystal of 100 Fourier-transform infrared spectrometer (Perkin-Elmer, Waltham, MA, USA) and dried at room temperature. Three spectra were collected from each sample. Spectra were acquired with 4 cm^{-1} spectral resolution.

2.7 | Cell toxicity assays

Mice midbrain N27 cells were grown in RPMI 1640 Medium (Thermo Fisher Scientific, Waltham, MA, USA) with 10% fetal bovine serum (FBS; Invitrogen, Waltham, MA, USA) in 96 well-plate (5000 cells per well) at 37°C under 5% CO_2. After 24 h, the cells were found to fully adhere to the wells reaching ~70% confluency. Next, 100 μL of the cell culture was replaced with 100 μL RPMI 1640 Medium with 5% FBS-containing protein samples. After 24 h of incubation with the sample of the protein aggregates, lactate dehydrogenase (LDH) assay (G1781, Promega, Madison, WI, USA) that was used to determine toxicity of protein aggregates. Absorption measurements were made in plate reader (Tecan, Mannedorf, Switzerland) at 490 nm. Every well was measured 25 times in different locations.

3 | RESULTS

3.1 | Morphological examination of protein aggregates

We first investigated the extent to which PAs with different lengths and saturation of FAs alter the morphology of lysozyme aggregates formed in their presence. For this, 200 μM of lysozyme was incubated in PBS at pH 3.0 in the absence of lipids (Lys), as well as in the presence of equimolar concentrations of PA-$C_{16:0}$, PA-$C_{18:0}$, and PA-$C_{18:1}$ at 65°C for 24 h. AFM imaging showed that in the absence of PA, lysozyme formed both short and long fibrils together with a large number of spherical oligomers (Figure 1). It should be noted that the amount of short fibrillar species with lengths of 100–200 nm was substantially greater than the concentration of long fibrils with lengths >200 nm. Both of these aggregates had

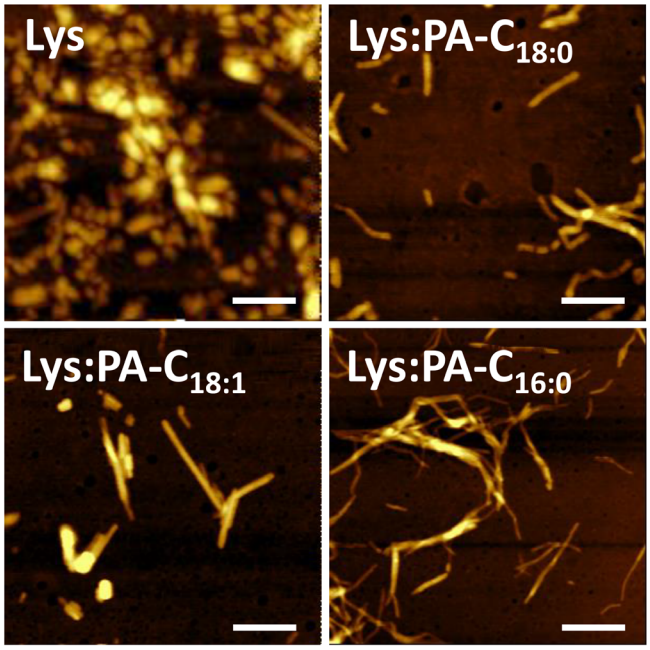

FIGURE 1 Length and saturation of FAs in PAs alter the morphology of lysozyme aggregates. AFM images of lysozyme aggregates formed in the lipid-free environment (Lys), as well as in the presence of PA-$C_{18:0}$ (Lys:PA-$C_{18:0}$), PA-$C_{18:1}$ (Lys:PA-$C_{18:1}$), and PA-$C_{16:0}$ (Lys:PA-$C_{16:0}$) formed at 65°C. Scale bars are 400 nm. AFM, atomic force microscopy; FAs, fatty acids; PAs, phosphatidic acids.

nearly identical heights (5–9 nm), suggesting that with time, short fibrils propagate into long fibrillar species (Figure S1). We also found that spherical oligomers exhibited slightly lower heights (4–6 nm) (Figure S1).

We found that in the presence of PA-$C_{18:0}$, very little if any oligomers were observed (Figure 1). We also observed the opposite distribution of short vs long fibrils. Specifically, nearly all fibrils observed in PA-$C_{18:0}$ were ≥200 nm. The same conclusions could be made for Lys:PA-$C_{18:1}$ and Lys:PA-$C_{16:0}$. We found that the vast majority of aggregates were long fibrils that had 7–10 nm in height (Figure S1). We also found that Lys:PA-$C_{18:0}$ and Lys:PA-$C_{18:1}$ were much thicker compared to Lys:PA-$C_{16:0}$ fibrils. At the same time, we found that Lys:PA-$C_{16:0}$ fibrils tended to intertwine forming fibril bundles, whereas such braiding propensity was not observed for Lys:PA-$C_{18:0}$ and Lys:PA-$C_{18:1}$ fibrils (Figure 1). These results demonstrated that the length and saturation of FAs of PA play an important role in the morphology of lysozyme aggregates formed in the presence of such phospholipids. We can also conclude that the length of the FAs in PS alters the propensity of filament association into higher-order amyloid structures. Furthermore, a very low concentration of short oligomeric species in Lys:PA-$C_{18:0}$, Lys:PA-$C_{18:1}$, and Lys:PA-$C_{16:0}$ compared to Lys suggests that phospholipids templated lysozyme aggregation, which results in a more uniform appearance of aggregates formed under such conditions.

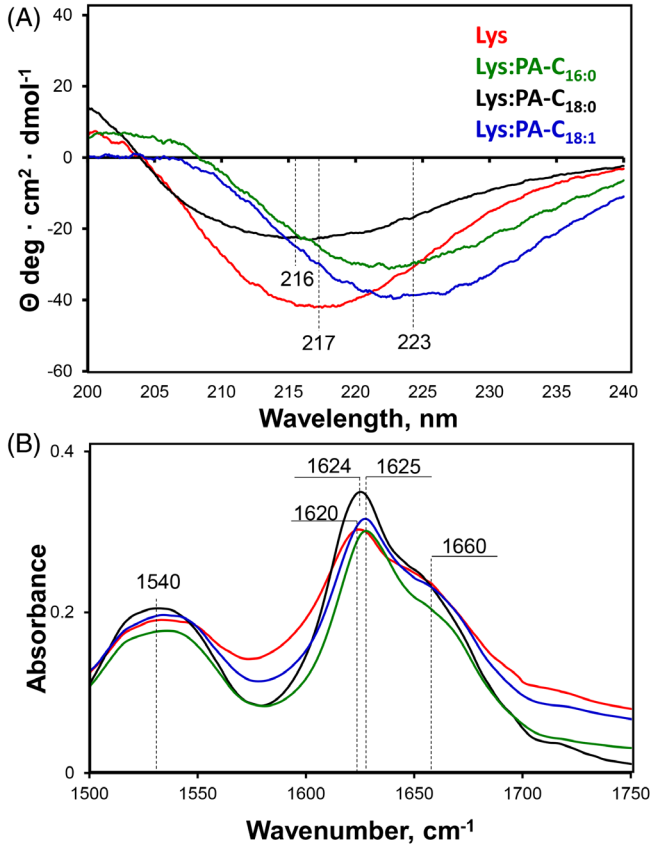

FIGURE 2 Length and saturation of FAs in PAs alter the secondary structure of lysozyme aggregates. CD (A) and IR (B) spectra acquired from lysozyme aggregates formed in the lipid-free environment (Lys), as well as in the presence of PA-$C_{18:0}$ (Lys:PA-$C_{18:0}$), PA-$C_{18:1}$ (Lys:PA-$C_{18:1}$), and PA-$C_{16:0}$ (Lys:PA-$C_{16:0}$) formed at 65°C. CD, circular dichroism; FAs, fatty acids; IR, infrared spectroscopy; PAs, phosphatidic acids.

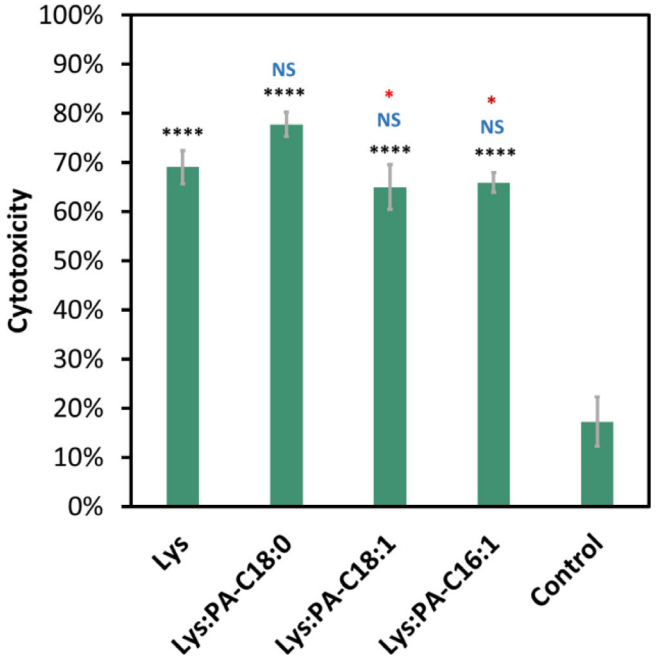

FIGURE 3 Histograms of LDH assay reveals differences between cell toxicity of Lys, Lys:PA-$C_{18:0}$, Lys:PA-$C_{18:1}$ and Lys:PA-$C_{16:0}$. Black asterisks show a significant level of differences between protein aggregates and the control; red asterisks show significance level of difference between Lys:PA-$C_{18:1}$, Lys:PA-$C_{16:0}$, and Lys:PA-$C_{18:0}$; * $p < .05$; **** $p < .0001$. NS shows an absence of statistical significance between Lys and lysozyme fibrils formed in the presence of different PAs. LDH, lactate dehydrogenase; PA, phosphatidic acid.

3.2 | Elucidation of the secondary structure of lysozyme aggregates formed in the presence of PA-$C_{16:0}$, PA-$C_{18:0}$, and PA-$C_{18:1}$

We utilized CD and infrared spectroscopy (IR) to determine the secondary structure of lysozyme aggregates formed in the lipid-free environment (Lys) and in the presence of PA-$C_{16:0}$, PA-$C_{18:0}$, and PA-$C_{18:1}$. CD spectra acquired from Lys exhibited a trough at ~ 217 nm indicating the dominance of β-sheet in the structure of Lys fibrils (Figure 2A).

These results are consistent with the IR spectra acquired from the Lys sample. In such spectra, amide I band can be used to determine the secondary structure of the analyzed protein samples. Specifically, α-helical species exhibit amide I at ~1640 cm^{-1}, whereas unordered proteins had amide I at ~1660 cm^{-1}. The presence of amide I at ~1623 cm^{-1} in the acquired IR spectra points on the predominance of parallel β-sheet, whereas the band at ~1690 cm^{-1} indicates the predominance of anti-parallel β-sheet in the protein specimens. We found that IR spectra acquired from Lys exhibited amide I band centered around 1620 cm^{-1}, which indicated the predominance of parallel β-sheet in the structure of Lys fibrils (Figure 2B). We also observed a small shoulder around 1660 cm^{-1}, which demonstrated the presence of a small amount of unordered protein in the Lys sample.

We also found that the trough in the CD spectra acquired from Lys:PA-$C_{18:0}$ was blue-shifted to 216 nm. Similar shifts were also observed in the IR spectra acquired from Lys:PA-$C_{18:0}$ compared to the IR spectrum of Lys (Figure 2A). Specifically, we found that the position of the amide I band shifted from 1620 to 1624 cm^{-1}. These spectroscopic changes point to a small difference in the secondary structure of Lys:PA-$C_{18:0}$ compared to lysozyme fibrils formed in the lipid-free environment. Furthermore, CD spectra acquired from Lys:PA-$C_{18:1}$ and Lys:PA-$C_{16:0}$ exhibited red shifts to 223 nm relative to the minimum in the CD spectrum of Lys (217 nm). IR spectra acquired from these samples exhibited an amide I band centered at 1625 cm^{-1}, which is substantially different from the position of amide I band in the IR spectrum of Lys (Figure 2B). Based on these results, we can conclude that the length and saturation of FAs in PA uniquely alter the secondary structure of lysozyme fibrils formed in their presence. We can also conclude that the secondary structure of such fibrils is different from the structure of lysozyme aggregates grown in the lipid-free environment.

3.3 | Toxicity of lysozyme aggregates formed in the presence of PA with different lengths and saturations of FAs

The question to ask is whether observed structural differences between Lys, Lys:PA-$C_{18:0}$, Lys:PA-$C_{18:1}$, and Lys:PA-$C_{16:0}$ have any biological significance. To answer this question, we investigate the extent to which these protein aggregates exert cell toxicity to mice midbrain N27 cell line (Figure 3).

LDH assay revealed a statistically significant difference between the toxicity exerted by Lys:PA-$C_{18:1}$, Lys:PA-$C_{16:0}$, and Lys:PA-$C_{18:0}$ fibrils. Thus, we can conclude that Lys:PA-$C_{18:0}$ fibrils were significantly more toxic than lysozyme aggregates formed in the presence of PA-$C_{18:1}$ and PA-$C_{16:0}$. These results demonstrate that both the length and saturation of FAs in PAs play an important role in the toxicity of lysozyme fibrils formed in the presence of such lipids. It should be noted that lysozyme fibrils formed in the lipid-free environment exhibited similar levels of cell toxicity compared to the aggregates formed in the presence of different PAs.

4 | DISCUSSION

The vast majority of amyloidogenic proteins either directly interact with lipid bilayers or are exposed to lipids in different organs and tissues.[7,33–35] For instance, α-Syn, a small protein that controls vesicle trafficking in synaptic clefts, instantaneously adopts α-helical secondary structure in the presence of lipid bilayers.[36] NMR and fluorescence studies revealed that α-Syn binds to lipids via electrostatic interactions that are taking place between charged head of lipids and polar amino acid residues of α-Syn.[37–40] In parallel, there are strong hydrophobic interactions developed between FAs' tails and hydrophobic amino acid residues of this protein.[37–40] Our group found that such lipid-protein complexes aggregate forming structurally different oligomers compared to those formed in the lipid-free environment.[26,41–43] Similar research findings were reported experimental results by Zhaliazka et al.[44] The researchers demonstrated that amyloid β 1–42 ($A\beta_{1\text{-}42}$) formed structurally different oligomers in the presence of phosphatidylcholine, cholesterol and CL. Furthermore, these oligomers exerted significantly higher cell toxicity compared to the oligomers formed by $A\beta_{1\text{-}42}$ in the lipid-free environment.[44] Zhang et al. demonstrated that low levels of anionic lipids promoted aggregation of islet amyloid polypeptide (IAPP).[45] However, zwitterionic lipid had no effect on the rate of IAPP aggregation. Finally, cholesterol at or below physiological levels significantly decelerated IAPP aggregation, as well as lowered the propensity of IAPP aggregates to cause membrane leakages.[45]

Injections of high concentrations of insulin in the skin derma, which are required for diabetes type 1 people, result in the high local concentration of insulin in confined areas surrounded by lipids.[46–50] Our group demonstrated that lipids could uniquely alter the rates of insulin aggregation.[21–26] Furthermore, the morphology and secondary structure of such aggregates are determined by the chemical structure of the lipid.[21–26] It was also found that saturation and length of FAs in PS, CL, and PA could strongly alter the aggregation rate and structure of insulin oligomers and fibrils.[21,23,24] Experimental results showed in the current study suggest saturation- and length-controlled structure of protein aggregates could be a general phenomenon attributed to the large group of amyloid proteins. Specifically, we found that length and saturation of FAs in PA altered both morphology and secondary structure of lysozyme aggregates. These structurally and morphologically different aggregates exert dissimilar cell toxicity.

One may expect that hydrogen binding between the lipid and proteins could play an important role in such interactions. In these cases, hydrogen bonds are developed between the aliphatic FAs of lipids and hydrophobic amino acid residues of proteins. Our results suggest infer that small differences in the hydrogen bonding between PA-$C_{18:0}$ and PA-$C_{18:1}$ with lysozyme can alter the thermodynamics of lipid: protein complex. This results in the structural and morphological differences between Lys:PA-$C_{18:0}$ and Lys:PA-$C_{18:1}$ fibrils. Differences in the thermodynamics of the lipid: protein complexes can also explain the discussed above differences between structures and morphologies of Lys:PA-C16:0 and Lys:PAC18:0 fibrils. Two CH_2 groups drastically alter the melting points of such lipids and consistently should alter the thermodynamics of the lysozyme–PA interactions. Elucidation of the thermodynamic properties of Lys:PA-C16:0, Lys:PA-C18:0, and LyL:PA-C18:1 complexes is the subject of a separate study.

Our findings are in agreement with the experimental results that were previously reported by Matveyenka et al. for insulin interactions with PAs. However, it was previously found that insulin:PA-$C_{16:0}$ fibrils exerted significantly lower cell toxicity compared to Lys:PA-$C_{18:0}$ and Lys:PA-$C_{18:1}$ aggregates, whereas the last two samples have statistically insignificant differences than insulin fibrils formed in the lipid-free environment.[24] These results show that toxicity of amyloid fibrils is determined not only be the structural properties of the lipid, but also by the structure of amyloidogenic proteins. These results also reveal the importance of hydrophobic interactions that take place between aliphatic side chains of phospholipids and non-polar amino acid residues of proteins in the protein aggregation. Using docking simulations, Holman et al. recently demonstrated that such hydrophobic forces primarily determined the interactions between insulin and FAs.[51] As a result, inulin–FAs complexes formed fibrils with opposite supramolecular chirality compared to those developed by insulin in the lipid-free environment. It was also found that hydrophobic interactions between insulin and FAs were strongly altered by the number of carbon atoms in FAs and the degree of their unsaturation.[51] The observed difference in the interactions of insulin and lysozyme with PAs suggested that two proteins have drastically different mechanisms of interactions with PAs that likely originated form differences in their amino acid sequences.

5 | CONCLUSIONS

Our results demonstrate that PA can uniquely alter lysozyme aggregation. Furthermore, saturation and length of FAs in PA determine

morphology, secondary structure, and toxicity of lysozyme fibrils formed in the presence of this phospholipid. These results suggest that structurally different lipids have dissimilar mechanisms of interactions with proteins.

AUTHOR CONTRIBUTIONS

Abid Ali: Conceptualization; investigation; methodology; validation; visualization. **Kiryl Zhaliazka:** Investigation; methodology; validation; visualization. **Aidan P. Holman:** Investigation; methodology; validation; visualization. **Dmitry Kurouski:** Conceptualization; funding acquisition; writing – original draft; writing – review and editing; project administration; supervision; resources.

FUNDING INFORMATION

This work was supported by National Institute of Health for the provided financial support (R35GM142869).

CONFLICT OF INTEREST STATEMENT

The authors declare on conflicts of interest.

PEER REVIEW

The peer review history for this article is available at https://www.webofscience.com/api/gateway/wos/peer-review/10.1002/prot.26622.

DATA AVAILABILITY STATEMENT

The data that support the findings of this study are available from the corresponding author upon reasonable request.

ORCID

Dmitry Kurouski https://orcid.org/0000-0002-6040-4213

REFERENCES

1. Knowles TP, Vendruscolo M, Dobson CM. The amyloid state and its association with protein misfolding diseases. *Nat Rev*. 2014;15(6):384-396.
2. Braak H, Braak E. Demonstration of amyloid deposits and neurofibrillary changes in whole brain sections. *Brain Pathol*. 1991;1(3):213-216.
3. Cherny RA, Legg JT, McLean CA, et al. Aqueous dissolution of Alzheimer's disease Abeta amyloid deposits by biometal depletion. *J Biol Chem*. 1999;274(33):23223-23228.
4. Chiti F, Dobson CM. Protein Misfolding, amyloid formation, and human disease: a summary of Progress over the last decade. *Annu Rev Biochem*. 2017;86(1):27-68.
5. Nelson R, Eisenberg D. Structural models of amyloid-like fibrils. *Adv Protein Chem*. 2006;73:235-282.
6. Hardy J, Selkoe DJ. The amyloid hypothesis of Alzheimer's disease: progress and problems on the road to therapeutics. *Science*. 2002;297(5580):353-356.
7. Ghosh U, Thurber KR, Yau WM, Tycko R. Molecular structure of a prevalent amyloid-beta fibril polymorph from Alzheimer's disease brain tissue. *Proc Natl Acad Sci U S A*. 2021;118(4):e2023089118.
8. Almeida CG, Takahashi RH, Gouras GK. Beta-amyloid accumulation impairs multivesicular body sorting by inhibiting the ubiquitin-proteasome system. *J Neurosci*. 2006;26(16):4277-4288.
9. Eisenberg DS, Sawaya MR. Structural studies of amyloid proteins at the molecular level. *Annu Rev Biochem*. 2017;86:69-95.
10. Gallardo R, Ranson NA, Radford SE. Amyloid structures: much more than just a cross-beta fold. *Curr Opin Struct Biol*. 2020;60:7-16.
11. Ghosh U, Yau WM, Collinge J, Tycko R. Structural differences in amyloid-beta fibrils from brains of nondemented elderly individuals and Alzheimer's disease patients. *Proc Natl Acad Sci U S A*. 2021;118(45):e2111863118.
12. Nelson R, Eisenberg D. Recent atomic models of amyloid fibril structure. *Curr Opin Struct Biol*. 2006;16(2):260-265.
13. Iadanza MG, Jackson MP, Hewitt EW, Ranson NA, Radford SE. A new era for understanding amyloid structures and disease. *Nat Rev Mol Cell Biol*. 2018;19(12):755-773.
14. Kurouski D, Lu X, Popova L, et al. Is supramolecular filament chirality the underlying cause of major morphology differences in amyloid fibrils? *J Am Chem Soc*. 2014;136(6):2302-2312.
15. Han S, Kollmer M, Markx D, Claus S, Walther P, Fandrich M. Amyloid plaque structure and cell surface interactions of beta-amyloid fibrils revealed by electron tomography. *Sci Rep*. 2017;7:43577.
16. Chauhan A, Ray I, Chauhan VP. Interaction of amyloid beta-protein with anionic phospholipids: possible involvement of Lys28 and C-terminus aliphatic amino acids. *Neurochem Res*. 2000;25(3):423-429.
17. Chi EY, Ege C, Winans A, et al. Lipid membrane templates the ordering and induces the fibrillogenesis of Alzheimer's disease amyloid-beta peptide. *Proteins*. 2008;72(1):1-24.
18. Galvagnion C, Brown JW, Ouberai MM, et al. Chemical properties of lipids strongly affect the kinetics of the membrane-induced aggregation of alpha-synuclein. *Proc Natl Acad Sci USA*. 2016;113(26):7065-7070.
19. Galvagnion C, Buell AK, Meisl G, et al. Lipid vesicles trigger alpha-synuclein aggregation by stimulating primary nucleation. *Nat Chem Biol*. 2015;11(3):229-234.
20. Zhaliazka K, Kurouski D. Nanoscale characterization of parallel and antiparallel beta-sheet amyloid beta 1-42 aggregates. *ACS Chem Neurosci*. 2022;13(19):2813-2820.
21. Matveyenka M, Rizevsky S, Kurouski D. Unsaturation in the fatty acids of phospholipids drastically alters the structure and toxicity of insulin aggregates grown in their presence. *J Phys Chem Lett*. 2022;13:4563-4569.
22. Matveyenka M, Rizevsky S, Pellois JP, Kurouski D. Lipids uniquely alter rates of insulin aggregation and lower toxicity of amyloid aggregates. *Biochim Biophys Acta Mol Cell Biol Lipids*. 2023;1868(1):159247.
23. Matveyenka M, Rizevsky S, Kurouski D. The degree of unsaturation of fatty acids in phosphatidylserine alters the rate of insulin aggregation and the structure and toxicity of amyloid aggregates. *FEBS Lett*. 2022;596(11):1424-1433.
24. Matveyenka M, Rizevsky S, Kurouski D. Length and unsaturation of fatty acids of phosphatidic acid determines the aggregation rate of insulin and modifies the structure and toxicity of insulin aggregates. *ACS Chem Neurosci*. 2022;13(16):2483-2489.
25. Matveyenka M, Rizevsky S, Kurouski D. Amyloid aggregates exert cell toxicity causing irreversible damages in the endoplasmic reticulum. *Biochim Biophys Acta Mol Basis Dis*. 2022;1868(11):166485.
26. Matveyenka M, Zhaliazka K, Rizevsky S, Kurouski D. Lipids uniquely alter secondary structure and toxicity of lysozyme aggregates. *FASEB J*. 2022;36(10):e22543.
27. Tanguy E, Wang QL, Moine H, Vitale N. Phosphatidic acid: from pleiotropic functions to neuronal pathology. *Front Cell Neurosci*. 2019;13:2.
28. Bader MF, Vitale N. Phospholipase D in calcium-regulated exocytosis: lessons from chromaffin cells. *Biochim Biophys Acta*. 2009;1791:936-941.
29. Stace CL, Ktistakis NT. Phosphatidic acid- and phosphatidylserine-binding proteins. *Biochim Biophys Acta*. 2006;1761:913-926.
30. Mizuno S, Sasai H, Kume A, et al. Dioleoyl-phosphatidic acid selectively binds to alpha-synuclein and strongly induces its aggregation. *FEBS Lett*. 2017;591(5):784-791.

31. Fitzner D, Bader JM, Penkert H, et al. Cell-type- and brain-region-resolved mouse brain Lipidome. *Cell Rep*. 2020;32(11):108132.
32. McMahon HT, Gallop JL. Membrane curvature and mechanisms of dynamic cell membrane remodelling. *Nature*. 2005;438(7068):590-596.
33. Pleyer C, Flesche J, Saeed F. Lysozyme amyloidosis—a case report and review of the literature. *Clin Nephrol Case Stud*. 2015;3:42-45.
34. Kayed R, Lasagna-Reeves CA. Molecular mechanisms of amyloid oligomers toxicity. *J Alzheimers Dis*. 2013;33(suppl 1):S67-S78.
35. Cerf E, Sarroukh R, Tamamizu-Kato S, et al. Antiparallel beta-sheet: a signature structure of the oligomeric amyloid beta-peptide. *Biochem J*. 2009;421(3):415-423.
36. O'Leary EI, Lee JC. Interplay between alpha-synuclein amyloid formation and membrane structure. *Biochim Biophys Acta Proteins Proteom*. 2019;1867(5):483-491.
37. Ysselstein D, Joshi M, Mishra V, et al. Effects of impaired membrane interactions on α-synuclein aggregation and neurotoxicity. *Neurobiol Dis*. 2015;79:150-163.
38. Bodner CR, Dobson CM, Bax A. Multiple tight phospholipid-binding modes of α-synuclein revealed by solution NMR spectroscopy. *J Mol Biol*. 2009;390(4):775-790.
39. Maltsev AS, Chen J, Levine RL, Bax A. Site-specific interaction between α-synuclein and membranes probed by NMR-observed methionine oxidation rates. *J Am Chem Soc*. 2013;135(8):2943-2946.
40. Bodner CR, Maltsev AS, Dobson CM, Bax A. Differential phospholipid binding of α-synuclein variants implicated in Parkinson's disease revealed by solution NMR spectroscopy. *Biochemistry*. 2010;49(5):862-871.
41. Rizevsky S, Matveyenka M, Kurouski D. Nanoscale structural analysis of a lipid-driven aggregation of insulin. *J Phys Chem Lett*. 2022;13(10):2467-2473.
42. Dou T, Kurouski D. Phosphatidylcholine and phosphatidylserine uniquely modify the secondary structure of alpha-synuclein oligomers formed in their presence at the early stages of protein aggregation. *ACS Chem Nerosci*. 2022;13(16):2380-2385.
43. Dou T, Zhou L, Kurouski D. Unravelling the structural Organization of Individual alpha-synuclein oligomers grown in the presence of phospholipids. *J Phys Chem Lett*. 2021;12(18):4407-4414.
44. Zhaliazka K, Kurouski D. Lipids uniquely Alter the secondary structure and toxicity of amyloid beta 1-42 aggregates. *FEBS J*. 2023;290:3203-3220. doi:10.1111/febs.16738
45. Zhang X, St Clair JR, London E, Raleigh DP. Islet amyloid polypeptide membrane interactions: effects of membrane composition. *Biochemistry*. 2017;56(2):376-390.
46. Kurouski D, Deckert-Gaudig T, Deckert V, Lednev IK. Structure and composition of insulin fibril surfaces probed by TERS. *J Am Chem Soc*. 2012;134(32):13323-13329.
47. Kurouski D, Postiglione T, Deckert-Gaudig T, Deckert V, Lednev IK. Amide I vibrational mode suppression in surface (SERS) and tip (TERS) enhanced Raman spectra of protein specimens. *Analyst*. 2013;138(6):1665-1673.
48. D'Souza A, Theis JD, Vrana JA, Buadi F, Dispenzieri A, Dogan A. Localized insulin-derived amyloidosis: a potential pitfall in the diagnosis of systemic amyloidosis by fat aspirate. *Am J Hematol*. 2012;87(11):E131-E132.
49. Gupta Y, Singla G, Singla R. Insulin-derived amyloidosis. *Indian J Endocrinol Metab*. 2015;19(1):174-177.
50. Shikama Y, Kitazawa J, Yagihashi N, et al. Localized amyloidosis at the site of repeated insulin injection in a diabetic patient. *Intern Med*. 2010;49(5):397-401.
51. Holman AP, Quinn K, Kumar R, Kmiecik S, Ali A, Kurouski D. Fatty acids reverse supramolecular chirality of insulin fibrils. *J Phys Chem Lett*. 2023;14:6935-6939.

SUPPORTING INFORMATION

Additional supporting information can be found online in the Supporting Information section at the end of this article.

How to cite this article: Ali A, Zhaliazka K, Holman AP, Kurouski D. Secondary structure and toxicity of lysozyme fibrils are determined by the length and unsaturation of phosphatidic acid. *Proteins*. 2023;1-7. doi:10.1002/prot.26622